

Investigating the static dipole polarizability of noble-gas atoms confined in impenetrable spheres and shells

J. A. Ludlow^{*} and Teck-Ghee Lee

Department of Physics, Auburn University, Auburn, Alabama 36849, USA

(Received 21 January 2015; published 20 March 2015)

The static dipole polarizability of noble-gas atoms confined by impenetrable spheres and spherical shells is studied using the B -spline random phase approximation with exchange. The general trend in dipole polarizabilities across the noble-gas sequence shows a decrease in the dipole polarizability as the volume of the confining impenetrable sphere is reduced and a large increase in the dipole polarizability for confinement by impenetrable spherical shells as the inner-shell radius is increased.

DOI: [10.1103/PhysRevA.91.032507](https://doi.org/10.1103/PhysRevA.91.032507)

PACS number(s): 31.15.ap, 32.10.Dk, 37.30.+i

I. INTRODUCTION

The study of atoms under confinement is a subject of long-standing interest; for a selection of reviews, see [1–6]. For many unconfined atoms, their polarizabilities are known to a high degree of accuracy, see [7] and [8]. An interesting question arises as to the effect of confinement on the polarizability of an atom.

The majority of studies investigating the polarizabilities of atoms under confinement have been carried out for hydrogen; see [9–11] for some early work and [12–18] for more recent calculations. For helium, an early calculation [19] has been followed by density functional [20], configuration-interaction [21], coupled-cluster [22], and variational [23] calculations with confining potentials studied including cylindrical [24] and spheroidal [25] potentials. For heavier systems, one-electron model potentials have been used to study the static dipole polarizability of alkali metals under hard-wall confinement [26] and Debye screening [27–29]. The static dipole polarizability and hyperpolarizability of beryllium were studied under harmonic, rectangular, and Gaussian confining potentials using a basis of explicitly correlated Gaussians [30]. For the polarizabilities of noble-gas atoms under hard-wall confinement, an early calculation studied the confined argon atom in a Thomas-Fermi model [31]. Hartree-Fock calculations [32–34] and a time-dependent density-functional theory [35] calculation have since been performed along the noble-gas sequence. The polarizabilities of confined noble gases are of interest in interpreting the density dependence of atomic polarizabilities [36] and studies of noble gas endofullerenes [37–39].

Here, nonrelativistic random phase approximation with exchange (RPAE) calculations of the static dipole polarizability are performed for noble-gas atoms under hard-wall confinement. The RPAE method [40–42] has been shown to give dipole polarizabilities accurate to within a few percent for the noble gases when compared to more sophisticated calculations [43], with relativistic effects having a small effect on polarizabilities for the noble gases [44].

The rest of the paper is structured as follows: Sec. II details the RPAE for the calculation of the static dipole polarizability and its numerical implementation using B splines. In Sec. III A, results are presented for the static dipole polarizabilities of hydrogen and noble-gas atoms confined by an impenetrable sphere. In Sec. III B the case of a spherical shell potential is investigated. Finally, Sec. IV concludes with a summary. Unless otherwise stated, atomic units are used throughout.

II. THEORY

A. Calculation of the dipole polarizability

For a hydrogen atom in the ground state, the static dipole polarizability can be calculated via the relation,

$$\alpha = 2 \sum_n \frac{|\langle np|z|1s\rangle|^2}{\varepsilon_{np} - \varepsilon_{1s}}. \quad (1)$$

For noble-gas atoms, electron correlation beyond the Hartree-Fock approximation plays an important role and must be accounted for. The dipole polarizability for noble-gas atoms will be calculated via the RPAE [40–42]. In the following equations for the RPAE vertex matrix element, the summation is over hole states, or states below the Fermi level ($\leq F$), and excited electron states above the Fermi level ($> F$).

For $v > F$ and $\mu \leq F$,

$$\begin{aligned} \langle v | A(\omega) | \mu \rangle &= \langle v | d | \mu \rangle + \left(\sum_{\substack{v' > F \\ \mu' \leq F}} - \sum_{\substack{\mu' > F \\ v' \leq F}} \right) \\ &\times \frac{(\langle v\mu' | V | v'\mu \rangle - \langle \mu'v | V | v'\mu \rangle)}{\omega - \varepsilon_{v'} + \varepsilon_{\mu'} + i\delta(1 - 2n_{v'})} \langle v' | A(\omega) | \mu' \rangle, \end{aligned} \quad (2)$$

and for $v \leq F$ and $\mu > F$,

$$\begin{aligned} \langle v | A(\omega) | \mu \rangle &= \langle v | d | \mu \rangle + \left(\sum_{\substack{v' > F \\ \mu' \leq F}} - \sum_{\substack{\mu' > F \\ v' \leq F}} \right) \\ &\times \frac{(\langle v\mu' | V | v'\mu \rangle - \langle \mu'v | V | v'\mu \rangle)}{\omega - \varepsilon_{v'} + \varepsilon_{\mu'} + i\delta(1 - 2n_{v'})} \langle v' | A(\omega) | \mu' \rangle, \end{aligned} \quad (3)$$

*Present address: AquaQ Analytics, Suite 5, Sturgeon Building, 9–15 Queen Street, Belfast, BT1 6EA; john@aquaq.co.uk

TABLE I. Static dipole polarizabilities for a hydrogen atom confined in an impenetrable sphere.

R	Present results	Kirkwood [18]	Buckingham [18]	Hylleraas [18]	Perturbation [14]
2.0	0.34255811	0.3401420	0.3401565	0.3425581	0.342558
4.0	2.37798233	2.2908060	2.3578222	2.3779823	2.377982
6.0	4.05814049	3.7054757	4.0471005	4.0581405	4.058140
8.0	4.45396473	3.9750587	4.4527846	4.4539647	4.453965

where $i\delta$ is an infinitesimal imaginary positive, and

$$n_{\nu'} = \begin{cases} 0 & \text{for } \nu' > F, \\ 1 & \text{for } \nu' \leq F. \end{cases} \quad (4)$$

Numerically, Eqs. (2) and (3) are a set of linear algebraic equations, which can be written in block matrix form,

$$\begin{pmatrix} x \\ y \end{pmatrix} = \begin{pmatrix} d \\ d \end{pmatrix} + \begin{pmatrix} V_1 & V_2 \\ V_2 & V_1 \end{pmatrix} \begin{pmatrix} \chi_1 & 0 \\ 0 & \chi_2 \end{pmatrix} \begin{pmatrix} x \\ y \end{pmatrix}, \quad (5)$$

where χ_1 and χ_2 are energy denominators, x and y represent $\langle \nu | A(\omega) | \mu \rangle$ for $\nu > F$, $\mu \leq F$ and $\nu \leq F$, $\mu > F$, respectively, d are the Hartree-Fock dipole matrix elements, and V_1 and V_2 are Coulomb matrices.

Once this equation has been solved for the RPA vertex, the dipole polarizability can be calculated via the relation

$$\alpha(\omega) = \sum_{\substack{\nu > F \\ \mu \leq F}} \frac{\langle \mu | d | \nu \rangle \langle \nu | A(\omega) | \mu \rangle}{\omega - \varepsilon_\nu + \varepsilon_\mu + i\delta} + \sum_{\substack{\nu \leq F \\ \mu > F}} \frac{\langle \mu | d | \nu \rangle \langle \nu | A(\omega) | \mu \rangle}{-\omega + \varepsilon_\nu - \varepsilon_\mu + i\delta}. \quad (6)$$

In this work the static dipole polarizability, $\omega = 0$, is calculated.

B. Numerical implementation

The Hartree-Fock equations will be solved for noble-gas atoms confined by a potential. Two forms of the confining potential will be compared here: first, an impenetrable spherical potential of the form

$$V_{\text{sph}}(r) = \begin{cases} 0 & \text{for } r < r_c, \\ \infty & \text{for } r \geq r_c, \end{cases} \quad (7)$$

where r_c is the radius of the confining potential; and second, an impenetrable spherical shell potential of the form

$$V_{\text{shell}}(r) = \begin{cases} \infty & \text{for } 0 \leq r \leq r_{\text{in}}, \\ 0 & \text{for } r_{\text{in}} < r < r_{\text{out}}, \\ \infty & \text{for } r \geq r_{\text{out}}, \end{cases} \quad (8)$$

where r_{in} is the inner radius and r_{out} is the outer radius of the spherical shell potential. As the radius of the confining potential may lie within the radius of the unconfined atom, it is necessary to incorporate potentials (7) and (8) into the numerical solution of the Hartree-Fock equations [45,46]. For all noble-gas atoms, the Hartree-Fock equations were solved using a cutoff radius of 30 a.u. and 6000 integration points. Note that for heavier atoms convergence of the Hartree-Fock equations

for small radii of the confining potential is more problematic. Results will be presented in this work down to the minimum radius of the confining potential for which convergence was obtained.

As polarizabilities of atoms can involve substantial contributions from continuum states, an efficient means of spanning the single-particle energy continuum is needed. Here, B -spline basis sets will be used [47,48]. B splines are piecewise polynomials defined on a particular knot sequence. For confinement by an impenetrable spherical potential, an exponential knot sequence is used of the form

$$t_1 = t_2 = \cdots = t_k = 0, \quad (9)$$

$$t_{n+1} = t_{n+2} = \cdots = t_{n+k} = r_c. \quad (10)$$

For $t_{k+1} \rightarrow t_n$,

$$t_i = r_0 \{\exp[\beta(i - k)] - 1\}, \quad (11)$$

$$\beta = \frac{\ln \left(\frac{r_c}{r_0} + 1 \right)}{(n + 1 - k)}, \quad (12)$$

where r_0 is a parameter which affects the smallest spacing of the knot sequence. For confinement by an impenetrable shell potential, an exponential knot sequence is used of the form

$$t_1 = t_2 = \cdots = t_k = r_{\text{in}}, \quad (13)$$

$$t_{n+1} = t_{n+2} = \cdots = t_{n+k} = r_{\text{out}}. \quad (14)$$

For $t_{k+1} \rightarrow t_n$,

$$t_i = r_{\text{in}} + r_0 \{\exp[\beta(i - k)] - 1\}, \quad (15)$$

$$\beta = \frac{\ln \left(\frac{(r_{\text{out}} - r_{\text{in}})}{r_0} + 1 \right)}{(n + 1 - k)}. \quad (16)$$

A value of $r_0 = 0.001$ with $n = 60$ splines of order $k = 9$ was used in this work.

TABLE II. Hartree-Fock energies for the 1s subshell of He confined in an impenetrable sphere.

R	E_{1s} (present work)	E_{1s} [52]
2.0	-0.65754880	-0.6593
4.0	-0.91252115	-0.9125
6.0	-0.91787985	-0.9174

TABLE III. Hartree-Fock energies for the $1s$, $2s$, and $2p$ subshells of Ne confined in an impenetrable sphere.

R	$1s$ (present work)	E_{1s} [52]	E_{2s} (present work)	E_{2s} [52]	E_{2p} (present work)	E_{2p} [52]
2.5	-32.41538078	-32.3831	-1.72747430	-1.7084	-0.62658124	-0.6076
3.0	-32.63113594	-32.5892	-1.84794644	-1.8239	-0.76329739	-0.7386
3.5	-32.71673490	-32.6763	-1.89664949	-1.8731	-0.81625604	-0.7924
4.0	-32.75109004	-32.7166	-1.91699524	-1.8963	-0.83731963	-0.8169

By expanding the radial wave functions in terms of B splines,

$$P_l(r) = \sum_i c_i^{(l)} B_i(r), \quad (17)$$

and substituting into the atomic Hamiltonian for hydrogen or the Hartree-Fock equation for noble-gas atoms,

$$H^{(l)} P_l(r) = \epsilon P_l(r), \quad (18)$$

a generalized eigenvalue problem is obtained for angular momentum l that can be solved to obtain a complete set of states suitable for the calculation of the atomic polarizabilities via Eqs. (1)–(6). The present calculations were carried out up to a maximum orbital angular momentum of $l = 10$. For confinement by an impenetrable spherical sphere, the boundary conditions $P_l(0) = P_l(r_c) = 0$ are implemented by removing the first and last splines, leaving $n - 2$ electron eigenstates for each orbital angular momentum l . Similarly, for confinement by an impenetrable spherical shell, the boundary conditions $P_l(r_{\text{in}}) = P_l(r_{\text{out}}) = 0$ are also implemented by removing the first and last splines, leaving $n - 2$ electron eigenstates for each orbital angular momentum l . For more details on the numerical implementation of the RPAE, see Chap. 2 of [49].

III. RESULTS

A. Static dipole polarizabilities of atoms confined by an impenetrable spherical potential

In order to benchmark the B -spline basis used in this work, Eq. (1) is used to calculate the static dipole polarizability of a hydrogen atom confined in an impenetrable sphere, with the results tabulated in Table I. Comparison with the results of perturbation-Hylleraas [18] and perturbation-numerical [14] calculations shows excellent agreement with the B -spline results. Comparison with the lower-bound Kirkwood [18] and Buckingham [18] results shows that the higher-order terms included in the Buckingham approximation [50] lead to a more accurate lower bound on the polarizability than the Kirkwood approximation [51].

To calculate the polarizability for multielectron atoms via the RPAE, bound states found from solving the Hartree-Fock equations are used to construct a complete set of states in a B -spline basis. Tables II and III compare the present Hartree-Fock subshell energies for helium and neon with the Roothaan-Hartree-Fock results of [52]. For the energy of the $1s$ subshell of helium there is good agreement between the calculations, while for the $1s$, $2s$, and $2p$ subshells of neon, the present subshell energies are more

TABLE IV. Static dipole polarizabilities calculated in the RPAE for noble-gas atoms confined in an impenetrable sphere.

R	He	Ne	Ar	Kr	Xe
1.8	0.27149963				
2.0	0.35985693				
2.5	0.60574486	0.99099895			
3.0	0.84391160	1.39793917	3.96443519		
3.5	1.03453905	1.74913386	5.36273398	6.64086248	
4.0	1.16491541	2.00968621	6.72840349	8.67526518	11.34371382
5.0	1.28514057	2.27781370	8.89416026	12.30276614	17.33513804
6.0	1.31534685	2.35591238	10.07330554	14.67047514	22.05689052
7.0	1.32113843	2.37303121	10.54979313	15.82775188	24.91468796
8.0	1.32206986	2.37613351	10.70305446	16.27562844	26.28682580
9.0	1.32220435	2.37663254	10.74468581	16.42077761	26.83277612
10.0	1.32222378	2.37671053	10.75476508	16.46192981	27.02021394
15.0	1.32223132	2.37673811	10.75782869	16.47631699	27.10088802
20.0	1.32223265	2.37674263	10.75792504	16.47654554	27.10156072
30.0	1.32223336	2.37674498	10.75797675	16.47666561	27.10188992
RPAE [40]		2.30	10.73	16.18	27.98
RRPA [44]	1.322	2.38	10.77	16.47	26.97
RCCSDT [43]		2.697	11.22	16.80	27.06
Hylleraas [53]	1.38376079				

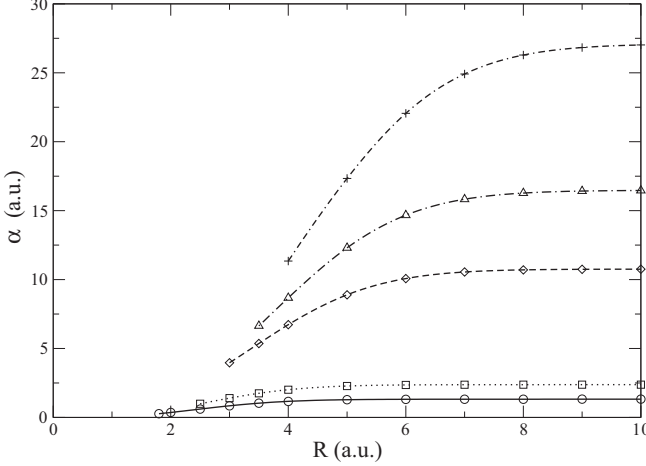


FIG. 1. Static dipole polarizabilities of the noble-gas sequence as a function of the confining potential radius. Solid line with circles, helium; dotted line with squares, neon; dashed line with diamonds, argon; dot-dashed line with triangles, krypton; dot-dot-dashed line with plus signs, xenon.

deeply bound than those of [52]. To further investigate this discrepancy, Roothaan-Hartree-Fock calculations for neon similar to those of [52] could be performed, examining convergence of the subshell energies with respect to both the orbital basis set size and the optimization of the basis set exponents.

Table IV contains static dipole polarizabilities calculated in the RPAAE for noble-gas atoms confined in an impenetrable sphere in comparison to unconfined polarizabilities, with the results displayed graphically in Fig. 1. It is seen that as the confining potential radius increases, the polarizability converges smoothly to closely agree with the relativistic RPA calculations of [44], demonstrating the small influence on the polarizabilities of relativistic effects. The nonrelativistic RPA calculations of [40] are slightly lower than the present results with the exception of xenon where the results of [40] are higher. The differences are within the estimated 5% uncertainty of the earlier calculations [40]. As the confining potential radius decreases, the polarizability decreases monotonically. Comparison with more precise Hylleraas calculations for helium [53] and relativistic coupled-cluster calculations for neon, argon, krypton, and xenon [43] shows that the nonrelativistic RPAAE method is able to recover the static dipole polarizability to within a few percent.

In Fig. 2, the present RPAAE polarizabilities for helium are compared to Hartree-Fock (HF) [32], density-functional theory (DFT) [20], and time-dependent density-functional theory (TDDFT) [35] calculations. The Hartree-Fock polarizabilities of [32] are larger than the current results and the other calculations at all box radii. The time-dependent density-functional theory polarizabilities of [35] are higher than the current results above a confining potential radius of 3 a.u. and fall off more strongly below a confining potential radius of 3 a.u. Excellent agreement with the present results is seen with the exact exchange, EXX, density-functional results

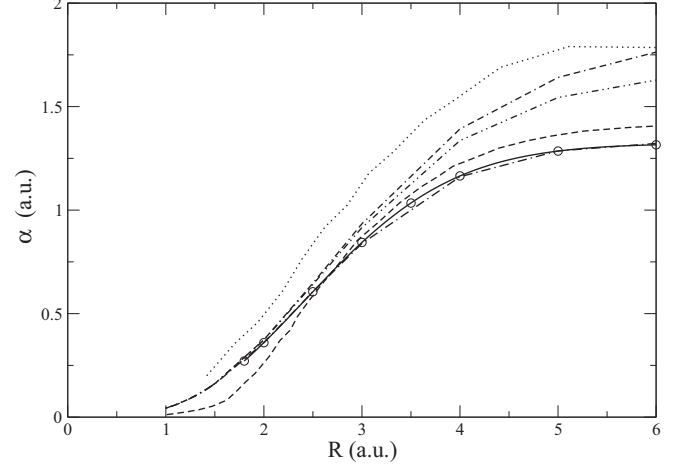


FIG. 2. Static dipole polarizabilities of helium as a function of the confining potential radius. Solid line with circles, present results; dotted line, HF [32] (digitized using g3data [54]); dashed line, TDDFT [35] (digitized using g3data [54]); dot-dashed line, DFT (EXX) [20]; dash-dot-dashed line, DFT (XO-LDA) [20]; dot-dot-dashed line, DFT (XC-LDA) [20].

of [20]. The exchange-only local-density approximation, XO-LDA, and exchange-correlation local-density approximation, XC-LDA, polarizabilities trend higher than the present results for larger confining potential radii, but agree better for smaller radii.

For neon, Fig. 3 compares the present RPAAE polarizabilities to Hartree-Fock [32] and time-dependent density-functional theory [35] calculations. Similarly to the case of helium, the Hartree-Fock polarizabilities of [32] are substantially higher than the current results. The time-dependent density-functional theory polarizabilities of [35] are in good agreement with the present results, with a distinctive sigmoidal shape seen in the polarizabilities as a function of the confining potential radius.

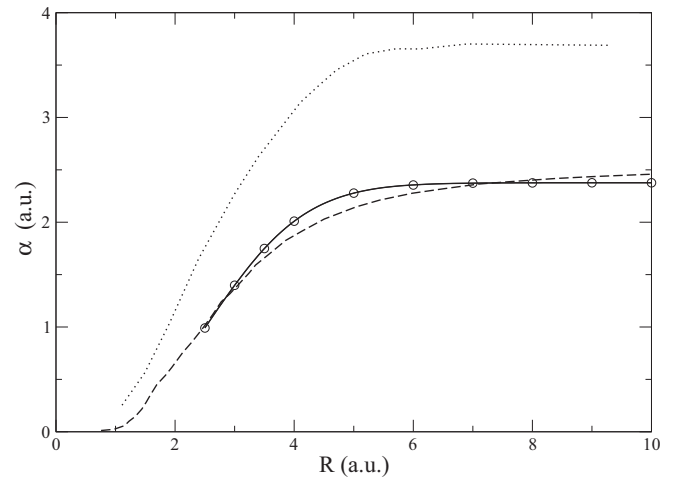


FIG. 3. Static dipole polarizabilities of neon as a function of the confining potential radius. Solid line with circles, present results; dotted line, [32] (digitized using g3data [54]); dashed line, [35] (digitized using g3data [54]).

TABLE V. Static dipole polarizabilities for hydrogen confined by an impenetrable spherical shell.

r_{in}	r_{out}	Present results	Perturbation [56]	Kirkwood [56]	Buckingham [56]
2.0	10.0	485.28323894	474.3865	420.8943	465.6254
4.0	10.0	1393.53470841	1372.0345	1043.0354	1352.7657

B. Static dipole polarizabilities of atoms confined by an impenetrable spherical shell potential

It has been demonstrated that confinement of noble-gas atoms by an impenetrable spherical potential leads to a monotonic decrease in the polarizability as the radius, and hence the volume, of the confining potential is reduced. A natural extension is to an impenetrable spherical shell potential; cf. Eq. (8). This potential may be of interest in the case of an atom confined by a negatively charged fullerene shell [55]. The polarizability of hydrogen confined in an impenetrable shell potential has been studied in [56–60]. Here, the confinement of helium and neon in a shell potential will be examined.

As for the case of an impenetrable spherical potential, the present calculations are first benchmarked for hydrogen. Table V compares the static dipole polarizabilities calculated using Eq. (1) against existing calculations [56] for hydrogen confined in a spherical shell potential of outer radius 10 a.u. with a varying inner-shell radius. There is seen to be close accord between the present results and those obtained in [56] using a perturbation numerical method and the Buckingham approximation [50]. As for confinement by an impenetrable spherical potential, results obtained using the Kirkwood approximation [51] tend to underestimate the polarizabilities. The polarizabilities increase rapidly as the inner-shell radius is increased.

RPAE calculations of the polarizabilities of helium and neon confined by a spherical shell potential of outer radius 10 a.u. with a varying inner-shell radius are presented in Table VI. The trend in the polarizabilities for helium and neon is similar to the case of hydrogen, with the polarizability for neon rising more strongly as the inner-shell radius is increased than that of helium.

TABLE VI. Static dipole polarizabilities calculated in the RPAE for helium and neon confined by an impenetrable spherical shell.

r_{in}	r_{out}	He	Ne
0.0	10.0	1.32222378	2.37671053
0.25	10.0	12.16238797	73.25472372
0.5	10.0	31.94196072	164.42341795
0.75	10.0	60.45733816	251.97880982
1.0	10.0	96.27102702	335.74822122
1.25	10.0	137.37472602	
1.5	10.0	181.62662627	
1.75	10.0	227.70588636	
2.0	10.0	274.39609861	
2.25	10.0	320.86226234	
2.5	10.0	366.59086983	

The increase of the polarizability of neon as the inner-shell radius is increased can be explored by examining the subshell energies; see Table VII. It is seen that a subshell rearrangement [61] occurs as the inner-shell radius is increased with the $2s$ subshell becoming more weakly bound than the $2p$ subshell as electrons are excluded from penetrating into the region near to the nucleus. As the inner-shell radius is increased the binding of the $2s$ orbital is decreased leading to a large increase in the polarizability.

IV. CONCLUSIONS

The static dipole polarizabilities of noble-gas atoms confined in impenetrable spherical spheres and impenetrable spherical shell potentials has been studied using the RPAE. Confinement in an impenetrable sphere leads to a decrease in the polarizability as the radius of the sphere is decreased. However, confinement by an impenetrable spherical shell potential leads to a large increase in the polarizability as the inner-shell radius is increased. This offers the potential of tuning the polarizability of an atomic system by confinement. Topics in the polarizabilities of confined multi-electron atoms that require further investigation include the influence of relativistic effects [62] and exploration of a range of confining potentials beyond the hard-wall confinement approximation, such as repulsive [63,64] or attractive [37] penetrable spherical shell potentials, with a view to exploring both higher-multipole polarizabilities and dynamic polarizabilities.

ACKNOWLEDGMENTS

We wish to acknowledge S. D. Loch for the generous provision of computing facilities and G. F. Gribakin for helpful discussions and suggestions.

TABLE VII. Hartree-Fock energies for the $1s$, $2s$, and $2p$ subshells of neon confined by an impenetrable spherical shell.

r_{in}	r_{out}	E_{1s}	E_{2s}	E_{2p}
0.0	10.0	-32.77243555	-1.93039045	-0.85040971
0.05	10.0	-11.67496109	-0.59126878	-1.30650997
0.25	10.0	-3.72928450	-0.24957000	-1.52410597
0.5	10.0	-2.18429623	-0.18295290	-1.23595070
0.75	10.0	-1.56730085	-0.14556270	-1.00631972
1.0	10.0	-1.22548285	-0.11740385	-0.84030892

- [1] W. Jaskólski, *Phys. Rep.* **271**, 1 (1996).
- [2] A. L. Buchachenko, *J. Phys. Chem. B* **105**, 5839 (2001).
- [3] J. P. Connerade and P. Kengkan, in *Proceedings of the Idea Finding Symposium, Frankfurt Institute for Advanced Studies*, edited by W. Greiner and J. Reinhardt (EP Systema, Debrecen, Hungary, 2004), pp. 35–46.
- [4] V. K. Dolmatov, A. S. Baltenkov, J. P. Connerade, and S. T. Manson, *Radiat. Phys. Chem.* **70**, 417 (2004).
- [5] *Theory of Confined Quantum Systems: Part One*, Advances in Quantum Chemistry, edited by J. R. Sabin, E. Brändas, and C. A. Cruz (Academic Press, New York, 2009), Vol. 57, pp. 1–334.
- [6] *Theory of Confined Quantum Systems: Part Two*, Advances in Quantum Chemistry, edited by J. R. Sabin, E. Brändas, and C. A. Cruz (Academic Press, New York, 2009), Vol. 58, pp. 1–297.
- [7] P. Schwerdtfeger, in *Atoms, Molecules and Clusters in Electric Fields: Theoretical Approaches to the Calculation of Electric Polarizability*, edited by G. Maroulis (World Scientific, London, 2006), Chap. 1, p. 1.
- [8] J. Mitroy, M. S. Safronova, and C. W. Clark, *J. Phys. B* **43**, 202001 (2010).
- [9] A. Michels, J. de Boer, and A. Bijl, *Physica (Amsterdam)* **4**, 981 (1937).
- [10] A. Sommerfeld and H. Welker, *Ann. Phys. (NY)* **424**, 56 (1938).
- [11] S. R. De Groot and C. A. Ten Seldam, *Physica (Amsterdam)* **12**, 669 (1946).
- [12] P. W. Fowler, *Mol. Phys.* **53**, 865 (1984).
- [13] A. Banerjee, K. D. Sen, J. Garza, and R. Vargas, *J. Chem. Phys.* **116**, 4054 (2002).
- [14] C. Laughlin, *J. Phys. B* **37**, 4085 (2004).
- [15] H. E. Montgomery, *Chem. Phys. Lett.* **352**, 529 (2002).
- [16] B. L. Burrows and M. Cohen, *Phys. Rev. A* **72**, 032508 (2005).
- [17] H. E. Montgomery and K. D. Sen, *Phys. Lett. A* **376**, 1992 (2012).
- [18] H. E. Montgomery, Jr. and V. I. Pupyshev, *Eur. Phys. J. H* **38**, 519 (2013).
- [19] C. A. Ten Seldam and S. R. De Groot, *Physica* **18**, 905 (1952).
- [20] S. Waugh, A. Chowdhury, and A. Banerjee, *J. Phys. B* **43**, 225002 (2010).
- [21] T. Sako and G. H. F. Diercksen, *J. Phys. B* **36**, 3743 (2003).
- [22] F. Holka, P. Neogrády, V. Kellö, M. Urban, and G. H. F. Diercksen, *Mol. Phys.* **103**, 2747 (2005).
- [23] S. Kar and Y. K. Ho, *Phys. Rev. A* **80**, 062511 (2009).
- [24] S. A. Ndengué, O. Motapon, R. L. Melingui Melono, and A. J. Etindele, *J. Phys. B* **47**, 015002 (2014).
- [25] A. Corella-Madueño, R. A. Rosas, J. L. Marín, and R. Riera, *Int. J. Quantum Chem.* **77**, 509 (2000).
- [26] S. H. Patil, K. D. Sen, and Y. P. Varshni, *Can. J. Phys.* **83**, 919 (2005).
- [27] N. Li-Na and Q. Yue-Ying, *Chin. Phys. B* **21**, 123201 (2012).
- [28] H. W. Li and S. Kar, *Phys. Plasmas* **19**, 073303 (2012).
- [29] Yue-Ying Qi and Li-Na Ning, *Phys. Plasmas* **21**, 033301 (2014).
- [30] K. Strasburger and P. Naciążek, *J. Phys. B* **47**, 025002 (2014).
- [31] C. A. Ten Seldam and S. R. De Groot, *Physica* **18**, 910 (1952).
- [32] P. K. Chattaraj and U. Sarkar, *J. Phys. Chem. A* **107**, 4877 (2003).
- [33] P. K. Chattaraj and U. Sarkar, *Chem. Phys. Lett.* **372**, 805 (2003).
- [34] P. K. Chattaraj, B. Maiti, and U. Sarkar, *Proc. Ind. Acad. Sci. (Chem. Sci.)* **115**, 195 (2003).
- [35] M. van Faassen, *J. Chem. Phys.* **131**, 104108 (2009).
- [36] M. Lallemand and D. Vidal, *J. Chem. Phys.* **66**, 4776 (1977).
- [37] S. A. Ndengé and O. Motapon, *J. Phys. B* **41**, 045001 (2008).
- [38] D. Sh. Sabirov and R. G. Bulgakov, *JETP Lett.* **92**, 662 (2010).
- [39] H. Yan, S. Yu, X. Wang, Y. He, W. Huang, and M. Yang, *Chem. Phys. Lett.* **456**, 223 (2008).
- [40] M. Ya. Amusia, N. A. Cherepkov, and S. G. Shapiro, *Zh. Eksp. Teor. Fiz.* **63**, 889 (1972) [Sov. Phys. JETP **36**, 468 (1973)].
- [41] M. Ya. Amusia and N. A. Cherepkov, *Case Stud. At. Phys.* **5**, 47 (1975).
- [42] M. Ya. Amusia, *Atomic Photoeffect* (Plenum Press, New York, 1990).
- [43] T. Nakajima and K. Hirao, *Chem. Lett.* **30**, 766 (2001).
- [44] W. R. Johnson, D. Kolb, and K. Huang, *At. Data Nucl. Data Tables* **28**, 333 (1983).
- [45] M. Ya. Amusia and L. V. Chernysheva, *Automated System for Atomic Structure Calculations* (Nauka, Leningrad, 1983).
- [46] L. V. Chernysheva, N. A. Cherepkov, and V. Radojević, *Comput. Phys. Commun.* **11**, 57 (1976).
- [47] H. Bachau, E. Cormier, P. Decleva, J. E. Hansen, and F. Martín, *Rep. Prog. Phys.* **64**, 1815 (2001).
- [48] C. De Boor, *A Practical Guide to Splines* (Springer, New York, 1978).
- [49] J. Ludlow, Ph.D. thesis, Queen's University Belfast, 2003.
- [50] R. A. Buckingham, *Proc. R. Soc. London, Ser. A* **160**, 94 (1937).
- [51] J. G. Kirkwood, *Phys. Z.* **33**, 57 (1932).
- [52] E. V. Ludeña, *J. Chem. Phys.* **69**, 1770 (1978).
- [53] G. Lach, B. Jeziorski, and K. Szalewicz, *Phys. Rev. Lett.* **92**, 233001 (2004).
- [54] g3data program, <http://www.frantz.fi/software/g3data.php>
- [55] J. A. Ludlow, Teck-Ghee Lee, and M. S. Pindzola, *J. Phys. B* **43**, 235202 (2010).
- [56] K. D. Sen, J. Garza, R. Vargas, and N. Aquino, *Phys. Lett. A* **295**, 299 (2002).
- [57] K. D. Sen, *J. Chem. Phys.* **122**, 194324 (2005).
- [58] B. L. Burrows and M. Cohen, *Mol. Phys.* **106**, 267 (2008).
- [59] N. Aquino, *Mol. Phys.* **107**, 2319 (2009).
- [60] B. L. Burrows and M. Cohen, *Mol. Phys.* **107**, 2323 (2009).
- [61] J. P. Connerade, V. K. Dolmatov, and P. A. Lakshmi, *J. Phys. B* **33**, 251 (2000).
- [62] J. P. Connerade and R. Semaoune, *J. Phys. B* **33**, 3467 (2000).
- [63] V. K. Dolmatov and J. L. King, *J. Phys. B* **45**, 225003 (2012).
- [64] V. K. Dolmatov, *J. Phys. B* **46**, 095005 (2013).